

Refereed Proceedings

The 12th International Conference on

Fluidization - New Horizons in Fluidization

Engineering

Engineering Conferences International

Year 2007

Study of Horizontal Sonic Gas Jets in
Gas-Solid Fluidized Beds

Matt Dawe*

Cedric Briens[†]

Franco Berruti[‡]

*The University of Western Ontario, mdawe@uwo.ca

[†]University of Western Ontario, cbriens@eng.uwo.ca

[‡]University of Western Ontario, fberruti@uwo.ca

This paper is posted at ECI Digital Archives.

http://dc.engconfintl.org/fluidization_xii/96

Dawe et al.: Horizontal Gas Jets in Fluidized Beds

STUDY OF HORIZONTAL SONIC GAS JETS IN GAS-SOLID FLUIDIZED BEDS

Matthew Dawe, Cedric Briens, and Franco Berruti

Department of Chemical and Biochemical Engineering

The University of Western Ontario

London, ON, Canada N6A 5B9

T: 1-519-661-2145; F: 1-519-661-3498; E: cbriens@uwo.ca

ABSTRACT

The objective of this study was to measure the jet boundaries of sonic gas jets in a gas-solid fluidized bed using triboelectric probes. An empirical correlation was developed to predict jet penetration based on the results. This correlation was compared with existing correlations developed for sub-sonic gas jets.

INTRODUCTION

Gas jets are critical in the operation of fluidized beds, and have, thus, been studied extensively in the literature. The main focus of these studies has been jets emitted from gas distributors such as perforated plates and spargers, leading to several correlations to predict the penetration depth of sub-sonic gas jets ([1](#), [2](#), [3](#), [4](#), [5](#), [6](#)).

The expansion angles of gas jets in fluidized beds have not been studied as extensively as the penetration length. De Michele et al. ([7](#)) and Behie et al. ([8](#)) reported jet half-angles of 13 – 18° for horizontal gas jets. Hinze ([9](#)) observed that the density of the jet fluid was of particular importance, and that the expansion angle decreased significantly when the jet fluid density was increased. Filla et al. ([10](#)) found that the expansion angle was larger for spherical particles than non-spherical particles, and that the angle increased with particle diameter and particle density. Cleaver et al. ([11](#)) observed that the jet expansion angle usually decreased with an increased jet velocity, especially for finer particles.

In processes such as fluid coking and jet milling, in which particle size control is required, attrition jets are used. These jets often operate at sonic or supersonic conditions in order to achieve desirable grinding efficiencies. Knowledge of sonic gas jet boundaries is necessary in order to prevent impact on reactor internals, or to optimize the arrangement of nozzles in cases which require jet impingement.

Currently, there is no study in the literature which determines the effectiveness of the existing gas jet correlations at predicting the jet penetration for sonic or supersonic jets. Furthermore, there is a lack of information regarding the development of a new correlation to predict the penetration of sonic gas jets.

The study by Dawe et al. (12) develops a triboelectric technique to measure jet boundaries in fluidized beds. The first objective of this study was to measure the jet penetration and expansion angle of sonic gas jets. The second objective was to test the existing correlations and their effectiveness in predicting the penetration depth of sonic gas jets. The final objective of this study was to develop a correlation to predict the jet penetration for sonic gas jets.

EQUIPMENT DESCRIPTION

Fluidized Bed System

The fluidized bed system used in this study is shown in Figure 1. Fluidization air flowed into the wind-box through sonic nozzles, which were used to control flow. The fluidization air was distributed by a perforated plate.

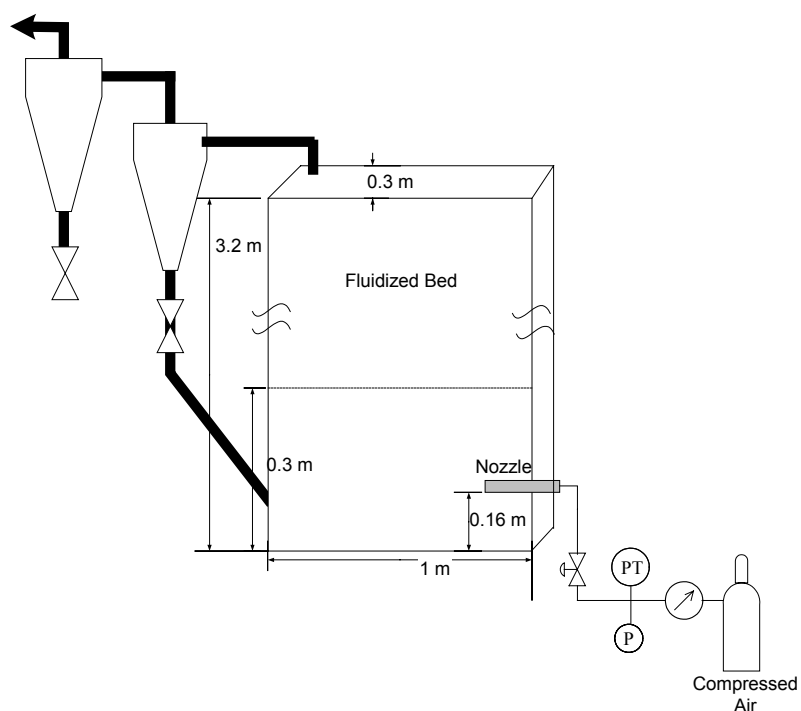


Figure 1. Fluidized bed system for gas jet tests

The bed was composed of one of three types of particles: fluid coke, silica sand, or glass beads.

Table 1. Bed particle properties for gas jet tests

| Bed Particle | d_{psm} (μm) | ρ_p (kg/m^3) | U_{mf} (m/s) | Φ (-) |
|--------------|-----------------------------|------------------------------|----------------|------------|
| Fluid Coke | 130 | 1400 | 0.0080 | 0.8 |
| Silica Sand | 180 | 2650 | 0.0263 | 0.8 |
| Glass Beads | 170 | 2500 | 0.0224 | 0.95 |

Injection Nozzles

Dawe et al.: Horizontal Gas Jets in Fluidized Beds

For each experiment, a nozzle injected gas horizontally into the fluidized particles. A constant mass flow rate of gas was supplied to the nozzle from a high-pressure cylinder. Controlling the supply pressure from the gas cylinder controlled the gas flow rate to the nozzle.

Three different types of nozzles were used in order to test the effects of nozzle geometry on the sonic gas jet boundaries. The first nozzle, Type A, was a convergent-divergent, Laval-type nozzle, similar to the one used by Benz (13). The second nozzle, Type B, was similar to the Type A nozzle except that it had a 10 mm long straight section added to the tip. The third nozzle, Type C, was a simple straight tube nozzle with a 25.4 mm long straight nozzle exit. The nozzles that were tested had diameters of 1.2 mm, 1.8 mm, 2.4 mm, or 4.3 mm. Three different gases: air, argon, and helium, were injected to test the effects of injected gas properties such as speed of sound, molar mass and viscosity on jet boundaries.

Triboelectric Probes

Twenty-eight triboelectric probes were made from plain insulated copper wire with a diameter of 1.5 mm and were installed so that they spanned the fluidized bed perpendicular to the nozzle flow, and were in the same horizontal plane as the injection nozzle. Further details on the probes and the method used to determine jet penetration length can be found in the study by Dawe et al. (12).

PART 1: JET PENETRATION DEPTH STUDY

Experimental Technique

For each test the bed was fluidized at an excess velocity, U_{ex} , of 0.039 m/s. An experimental matrix was developed so that the effects of injection gas flow rate (velocity), injection gas type, nozzle type, nozzle diameter and solids type could be studied independently from one another. Jet penetration was measured during each test using the triboelectric probes.

Results and Discussion

As expected, when the nozzle size was increased, the jet penetrated further, as seen in Figure 2. This is a result of the increased gas mass flow rate with the larger nozzles. These results were also observed by Merry (2) for sub-sonic jets.

Figure 2 also shows that Nozzle A penetrated further than Nozzle B and Nozzle C of the same throat diameter. The convergent-divergent geometry caused an increase in jet length when compared to the straight tube nozzle, while the addition of a straight tube section to the end of the shaped nozzle caused a decrease in jet length.

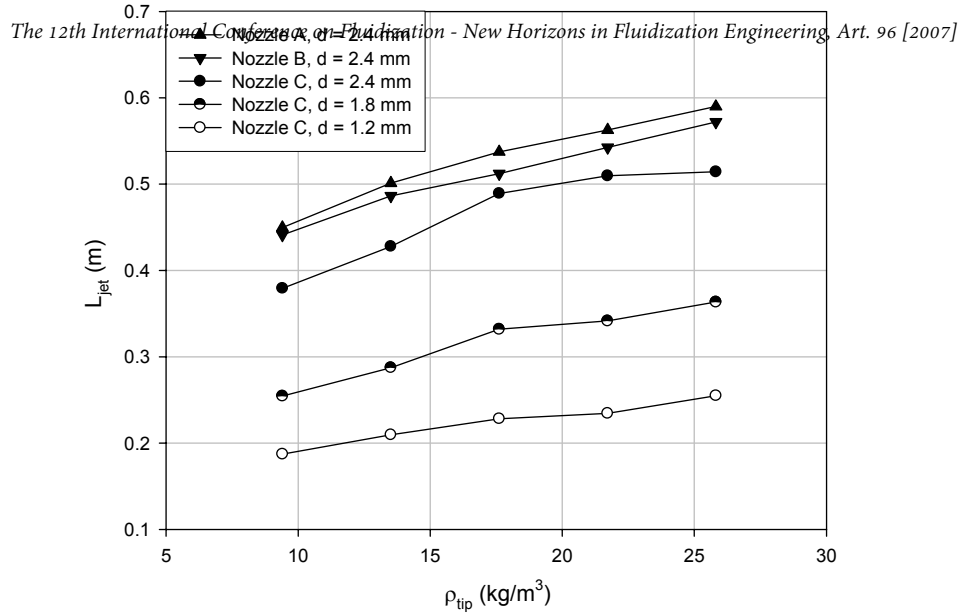


Figure 2. Effect of nozzle geometry, nozzle scale, and jet density on L_{jet} (Fluidized bed particles: coke; Injection gas: air)

When the upstream pressure of the jet gas was increased, the gas density at the nozzle tip and the gas mass flow rate both increased. This also resulted in a longer jet, (Figure 2). The same trend was observed in the literature for sub-sonic jets.

It was observed that jet penetration decreased nearly linearly as d_{psm}/Φ increased. Therefore, the particle size and shape were both important factors when considering the penetration of the jet. This trend is consistent with the sub-sonic gas jet observations of Musmarra (14), who noted that jet penetration decreased with increasing particle size.

The effect of d_{psm}/Φ was analyzed more closely. To begin, it has been observed by Dawe et al. (12) that an increase in gas entrainment causes a decrease in jet penetration. This relationship exists because as gas is entrained into the jet, more solids are entrained along with the gas. The jet then has to spend energy on accelerating the additional gas and solids; therefore, energy dissipation in the jet occurs faster, and the jet does not penetrate as far into the bed. The reason gas is entrained into the jet is due to the lower pressure that occurs in the jet relative to the bed pressure. The gas that flows into the jet flows through a fixed bed of defluidized particles which surrounds the jet. The existence of this defluidized region has been visually confirmed by Hulet et al. (15).

Ergun (16) proposed an equation for the pressure drop through a fixed bed. By using this equation in combination with the equation developed by Chen (17), it can be shown that:

$$F_{g,e} \propto \frac{\varepsilon^3}{1-\varepsilon} \Phi d_p \propto \frac{d_p}{\Phi} \quad (1)$$

So, it can be seen that as d_p/Φ increases, the entrained gas flow rate into the jet also increases, thus explaining the decrease in jet penetration.

It was observed that for a constant jet velocity, the jet penetration increased as the gas density was increased. This is logical since the jet with the greater gas density had a higher mass flow rate at the same velocity, which resulted in greater jet momentum. This trend was also observed by Vaccaro et al. (18) for sub-sonic jets.

Correlations from the literature (1, 2, 3, 4, 5, 6) were applied to predict L_{jet} for sonic gas jets, and the predictions were compared to the experimental values. While the correlations from Merry (2) and Ariyapadi et al. (6) performed the best with R^2 values of 0.71 and 0.89, respectively, there was significant scatter associated with the predicted values. Modifying the coefficient and exponents of these correlations could not provide a good correlation.

Since none of the existing correlations performed adequately for the sonic gas jet data, a new empirical correlation was developed that used the nozzle diameter, the equivalent speed of sound in the injection gas, and the density of the injection gas at the nozzle tip and two particle-specific empirical constants. The correlation fit the experimental data with a R^2 value of 0.94, and therefore, was an improvement over the existing gas jet correlations.

$$\frac{L_{jet}}{d} = \alpha \cdot U_{sound,eq}^{0.488} \cdot \rho_{tip}^{0.329} + \frac{\beta}{d} \quad (2)$$

The values of α and β for each solids type are listed below in Table 2.

Table 2. Values of empirical constants for gas jet correlation

| Bed Particle Type | α | β |
|-------------------|----------|---------|
| Coke | 5.53 | 0.001 |
| Glass Beads | 3.55 | 0.101 |
| Silica Sand | 2.13 | 0.175 |

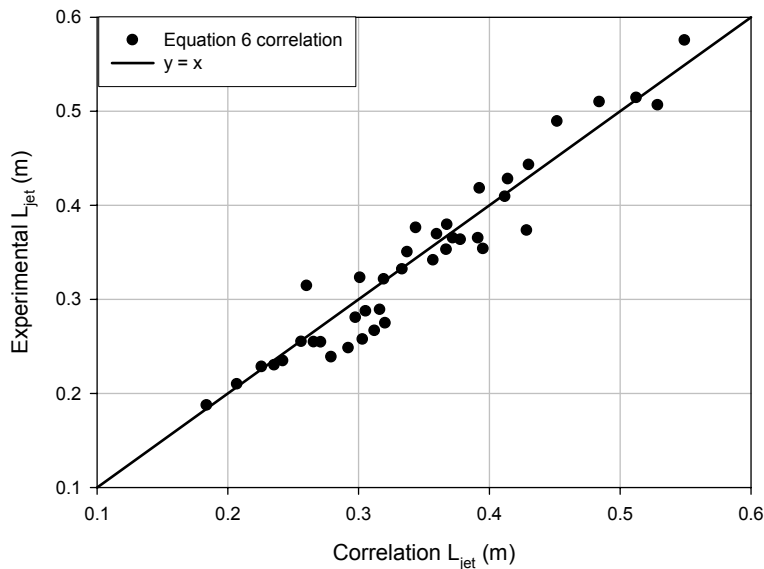


Figure 3. Comparison of new empirical correlation with experimental data

PART 2: EXPANSION ANGLE STUDY

All tests in this section were run with silica sand as the bed solids. For each set of conditions to be studied, the triboelectric probes were started with their measuring section along the jet axis. The probes were then moved outwards from the jet axis at 2 degree intervals until a triboelectric signal could no longer be detected.

Once the triboelectric signals were obtained, a power spectrum analysis was performed between the frequencies of 0 and 200 Hz, excluding 55 to 65 Hz. The average power of the signal in this frequency range was calculated for each probe in the expansion region of the jet for each angle. The mean value of all of the average power values was calculated, and plotted versus the angle (Figure 4). Figure 4 shows that the power decreases steadily with the angular position of the triboelectric probe until the probes moves from the jet into the bed and the signal becomes approximately constant.

As expected, when the gas mass flow rate (W_g) was increased, the expansion angle increased due to the increased pressure inside the nozzle. It was also observed that the geometry of the nozzle did not have much of an effect on the expansion angle. However, the scale of the nozzle did have an effect on the expansion angle of the jet. When operated at the same gas mass flow rate, Nozzle C with a diameter of 4.3 mm had a significantly smaller expansion angle than Nozzle C with a diameter of 2.4 mm. This occurred because the larger nozzle had a lower density at the nozzle tip. Further testing of the different sized nozzles, while keeping the gas mass flux (W_g/A_{nozzle}) constant, would help develop a clearer understanding of the effects of scale on the jet expansion angle.

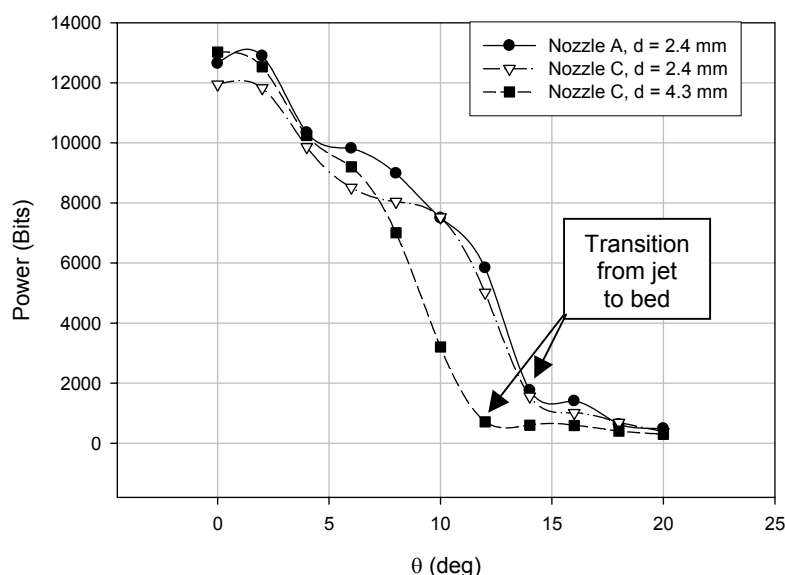


Figure 4. Sample results of power spectrum analysis for $W_g = 0.008$ kg/s

Increasing the density of the injection gas reduced the expansion angle: the angle was 18 degrees for a density of 0.2 kg/m^3 and 13° for a density of 1.6 kg/m^3 . This observation was supported by the findings of Hinze (9) for sub-sonic jets. For the same mass flow rate of gas, the helium jets had a significantly larger angle than the

air and argon jets. This is due to the fact that helium had a much greater jet velocity at the nozzle tip (due to its higher sonic velocity).

CONCLUSIONS

It was found that none of the existing correlations, developed for sub-sonic jets, could accurately predict the penetration depth of sonic jets. A new correlation was developed for sonic jets and provided more accurate predictions. It involved the diameter of the nozzle, the equivalent speed of sound of the gas, the density of the gas at the nozzle tip, and two empirical constants.

The expansion angle of sonic gas jets was measured using the triboelectric probes. A power spectrum analysis of the triboelectric signals was required to obtain the experimental expansion angle. The expansion angle was found to increase when the gas mass flow rate was increased, and decrease when the nozzle diameter was increased. Also, the observed expansion angle decreased when the injection gas density was increased.

ACKNOWLEDGEMENTS

The authors wish to gratefully acknowledge the financial support of Syncrude Canada Ltd. Support from the Natural Sciences and Engineering Research Council of Canada (NSERC), in the form of a grant to Cedric Briens and Franco Berruti, and of a scholarship to Matt Dawe is also gratefully acknowledged. A special thank you is due to Jennifer McMillan for her invaluable assistance with experiments.

NOMENCLATURE

| | |
|----------------|--|
| ALR | air-to-liquid ratio (wt%) |
| C_g | nozzle geometry parameter (-) |
| d | nozzle diameter (m) |
| d_p | Sauter-mean particle diameter (m) |
| g | acceleration due to gravity (m/s^2) |
| G_L | superficial liquid mass velocity at the nozzle exit (kg/m^2-s) |
| $F_{g,e}$ | mass flow rate of entrained gas (kg/s) |
| Fr | Froude number (-) |
| L_{jet} | jet penetration length (m) |
| M | molar mass (kg/kgmol) |
| P | upstream injection gas pressure (kPa) |
| S | mean slip velocity ratio (-) |
| U | velocity (m/s) |
| U_{ex} | excess fluidization velocity (m/s) |
| U_g | superficial fluidization gas velocity (m/s) |
| U_{mf} | minimum superficial fluidization velocity (m/s) |
| $U_{sound,eq}$ | equivalent speed of sound (m/s) |
| W_g | mass flow rate of gas to the nozzle (kg/s) |

Greek Letters

| | |
|------------------|---|
| α | empirical correlation for jet penetration correlation (-) |
| β | empirical correlation for jet penetration correlation (-) |
| ΔP_{fix} | pressure drop in fixed bed (kPa/m) |

| | |
|---------------------|--|
| ε_{bed} | fluidized bed void fraction (-) |
| ε' | mean void fraction based on slip conditions (-) |
| ε_{mf} | fluidized bed void fraction at minimum fluidization (-) |
| μ_g | gas viscosity (kg/m-s) |
| Φ | particle sphericity (-) |
| μ_g | gas viscosity (Pa.s) |
| ρ_f | fluid density (kg/m ³) |
| ρ_g | injection gas density at bed conditions (kg/m ³) |
| ρ_{tip} | injection gas density at nozzle tip (kg/m ³) |
| θ | jet expansion half angle (degrees) |

REFERENCES

- (1) Zenz, F.A., "Bubble formation and grid design", I. Chem. E. Symp. Series **30**, 136-139 (1968).
- (2) Merry, J.D., "Penetration of a horizontal gas jet into a fluidized bed", Trans. Instrn. Chem. Eng. **49**, 189-195 (1971).
- (3) Yates, J.G., Cobbinah, S.S., Cheesman, D.J., Jordan, S.P., "Particle attrition in fluidized beds containing opposing jets", AIChE Symp. Series **281**, 13-19 (1988).
- (4) Benjelloun, F., Liegeois, R., Vanderschuren, J., "Penetration length of horizontal gas jets into atmospheric fluidized beds", Proc. Fluidization-VIII, J-F. Large and C. Laguerie Eds., Engineering Foundation, N.Y., 239-246 (1995).
- (5) Hong, R., Li, H., Li, H., Wang, Y., "Studies on inclined jet penetration length in a gas-solid fluidized bed", Powder Tech. **92**, 205-212 (1997).
- (6) Ariyapadi, S., Berruti, F., Briens, C., McMillan, J., Zhou, D., "Horizontal penetration of gas-liquid spray jets in gas-solid fluidized beds", Intl. J. Chem. Reactor Eng. **2**, Article A22 (2004).
- (7) De Michele, G., Elia, A., Massimilla, L., "The interaction between jets and fluidized beds", Ing. Chim. Ital. **12**, 155-162 (1976).
- (8) Behie, L., Bergougnou, M.A., Baker, C.J., "Heat transfer from a grid in a large fluidized bed", Can. J. Chem. Eng. **53**, 25-30 (1975).
- (9) Hinze, J.O., "Turbulence", McGraw-Hill, New York (1975).
- (10) Filla, M., Massimilla, L., Vaccaro, S., "Gas jets in fluidized beds: The influence of particle size, shape and density on gas and solids entrainment", Int. J. Multiphase Flow **9**, 259-267 (1983).
- (11) Cleaver, J.A.S., Ghadiri, M., Tuponogov, V.G., Yates, J.G., Cheesman, D.J., "Measurement of jet angles in fluidized beds", Powder Tech. **85**, 221-226 (1995).
- (12) Dawe, M., Briens, C., Berruti, F., "Study of gas-liquid jet boundaries in a gas-solid fluidized bed", To be submitted to Powder Tech. (2006a).
- (13) Benz, M., Herold, H., Ulfik, B., "Performance of a fluidized bed jet mill as a function of operating parameters", Int. J. Miner. Process. **44**, 507-519 (1996).
- (14) Musmarra, D., "Influence of particle size and density on the jet penetration length in gas fluidized beds", Ind. Eng. Chem. Res. **39**, 2612-2617 (2000).
- (15) Hulet, C., Briens, C., Berruti, F., McMillan, J., Chan, E.W., "Flow patterns of entrained solids into a submerged gas jet: effect of a shroud", Submitted to the Int. J. Chem. Reactor Eng., (2006).
- (16) Ergun, S., Chem. Eng. Prog. **48**, 89 (1952).
- (17) Chen, J.J.J., IEC Res. **26**, 464 (1987).
- (18) Vaccaro, S., Musmarra, D., Petrecca, M., "Evaluation of the jet penetration depth in gas-fluidized beds by pressure signal analysis", Int. J. Multiphase Flow **23**, 689-698 (1997).